

# Robo2 is required for establishment of a precise glomerular map in the zebrafish olfactory system

Nobuhiko Miyasaka<sup>1</sup>, Yuki Sato<sup>1</sup>, Sang-Yeob Yeo<sup>2,\*</sup>, Lara D. Hutson<sup>3,†</sup>, Chi-Bin Chien<sup>3</sup>, Hitoshi Okamoto<sup>2,4</sup> and Yoshihiro Yoshihara<sup>1,‡</sup>

<sup>1</sup>Laboratory for Neurobiology of Synapse, RIKEN Brain Science Institute, 2-1 Hirosawa, Wako-shi, Saitama 351-0198, Japan

<sup>2</sup>Laboratory for Developmental Gene Regulation, RIKEN Brain Science Institute, 2-1 Hirosawa, Wako-shi, Saitama 351-0198, Japan

<sup>3</sup>Department of Neurobiology and Anatomy, University of Utah Medical Center, Salt Lake City, UT 84132, USA

<sup>4</sup>Core Research for Evolutional Science and Technology (CREST), Japan Science and Technology Corporation (JST), 3-4-5 Nihonbashi, Chuo-ku, Tokyo 103-0027, Japan

\*Present address: Laboratory of Molecular Genetics, NICHD, NIH, Bethesda, MD 20892, USA

†Present address: Department of Biology, Williams College, Williamstown, MA 01267, USA

‡Author for correspondence (e-mail: yoshihara@brain.riken.go.jp)

Accepted 14 January 2005

Development 132, 1283-1293

Published by The Company of Biologists 2005

doi:10.1242/dev.01698

## Summary

Olfactory sensory neurons (OSNs) expressing a given odorant receptor project their axons to specific glomeruli, creating a topographic odor map in the olfactory bulb (OB). The mechanisms underlying axonal pathfinding of OSNs to their precise targets are not fully understood. Here, we demonstrate that Robo2/Slit signaling functions to guide nascent olfactory axons to the OB primordium in zebrafish. *robo2* is transiently expressed in the olfactory placode during the initial phase of olfactory axon pathfinding. In the *robo2* mutant, *astray* (*ast*), early growing olfactory axons misroute ventromedially or posteriorly, and often penetrate into the diencephalon without reaching the OB primordium. Four zebrafish Slit homologs are expressed in regions adjacent to the olfactory axon

trajectory, consistent with their role as repulsive ligands for Robo2. Masking of endogenous Slit gradients by ubiquitous misexpression of Slit2 in transgenic fish causes posterior pathfinding errors that resemble the *ast* phenotype. We also found that the spatial arrangement of glomeruli in OB is perturbed in *ast* adults, suggesting an essential role for the initial olfactory axon scaffold in determining a topographic glomerular map. These data provide functional evidence for Robo2/Slit signaling in the establishment of olfactory neural circuitry in zebrafish.

Key words: Axon guidance, Pioneer neurons, Glomerulus, Transgenic zebrafish

## Introduction

In vertebrate sensory systems, peripheral sensory neurons make precise synaptic connections with second-order neurons in the brain to create an internal neural representation of external stimuli. In the olfactory system, individual olfactory sensory neurons (OSNs) express only one odorant receptor (OR) from a repertoire of ~1,000 genes in rodents and ~100 genes in fish (Mombaerts, 1999). In mice, OSNs expressing a given OR are widely distributed within the olfactory epithelium (OE), yet they converge their axons onto a few specific glomeruli in the olfactory bulb (OB), creating an odor map (Ressler et al., 1994; Vassar et al., 1994; Mombaerts et al., 1996).

This feat is accomplished by sophisticated processes of axon guidance and synapse formation during development, which can be divided into at least three steps. First, nascent olfactory axons exit the OE, coalesce to form fascicles, and grow toward the OB primordium at the rostral tip of the telencephalon. Second, upon reaching the OB primordium, the olfactory axons defasciculate tangentially and sort out into smaller subsets toward restricted domains of the OB. Third, the olfactory axons

make synaptic connections in target glomeruli with the dendrites of OB projection neurons and interneurons. What molecules are responsible for the establishment of the topographic odor map? Genetic deletions or substitutions of specific OR genes in mice have suggested that the ORs themselves play an instructive role in glomerular targeting (Mombaerts et al., 1996; Wang et al., 1998; Feinstein and Mombaerts, 2004; Feinstein et al., 2004). Several cell recognition molecules have been implicated as guidance ligands and receptors for OSN axons that function at a series of choice points along the navigation course from the OE to the target glomeruli (St John et al., 2002). For instance, semaphorin 3A and ephrin-As have been shown to be involved in axon sorting within the olfactory nerve layer and in axon termination onto precise glomerular positions, respectively (Schwartz et al., 2000; Taniguchi et al., 2003; Cutforth et al., 2003). However, it remains largely unknown how the early growing olfactory axons are precisely guided to the OB primordium. Roundabouts (Robos) and Slits, chemorepulsive receptors and ligands, appear to be good candidates to achieve this function in the light of their spatiotemporal expression

patterns in the developing olfactory system (Yuan et al., 1999; Lee et al., 2001; Marillat et al., 2002).

Robos are evolutionarily conserved transmembrane glycoproteins belonging to the immunoglobulin (Ig) superfamily (Kidd et al., 1998; Sundaresan et al., 1998; Zallen et al., 1998). Robo was originally identified from studies of *Drosophila* mutants in which axons misroute at the midline in the ventral nerve cord (Seeger et al., 1993). *Drosophila* Robo protein prevents commissural axons from inappropriately recrossing the midline by sensing the repulsive ligand Slit secreted from the midline glia (Kidd et al., 1998; Kidd et al., 1999). In vertebrates, the roles of Robo/Slit repulsive signaling have been implicated in axon pathfinding of various types of neurons (Bagri et al., 2002; Nguyen-Ba-Charvet et al., 2002; Plump et al., 2002; Knöll et al., 2003; Long et al., 2004). We have previously shown that the zebrafish mutant *astray* (*ast*) exhibits deviation of retinal axons from their normal route, and that *ast* is defective in the gene encoding Robo2 (Fricke et al., 2001; Hutson and Chien, 2002).

Here, we demonstrate, by using *ast* mutants and Slit2-overexpressing zebrafish, that Robo/Slit signaling is required for proper navigation of the early growing olfactory axons toward the OB primordium. Furthermore, we propose that the establishment of a sound glomerular map in the adult OB requires the precise formation of the initial axon scaffold, which is mediated by Robo2 at early developmental stages.

## Materials and methods

### Fish maintenance

Zebrafish, *Danio rerio*, were maintained and embryos were collected essentially as described (Westerfield, 1995). Embryos were staged according to hours postfertilization (hpf) at 28.5°C and morphological criteria (Kimmel et al., 1995). Collected embryos were maintained in 1/3 Ringer's solution (39 mM NaCl, 0.97 mM KCl, 1.8 mM CaCl<sub>2</sub>, 1.7 mM Hepes at pH 7.2) supplemented with 100 units/ml penicillin and 100 µg/ml streptomycin. In some cases, 0.002% phenylthiourea was added after 12 hpf to prevent pigmentation.

### Generation of transgenic zebrafish

A bacterial artificial chromosome (BAC) clone containing the zebrafish olfactory marker protein (OMP) gene was isolated from Down-to-the-Well BAC pools (Genome Systems). Roughly 6-kb and 2-kb fragments upstream of the OMP translation start site were subcloned into pEGFP-1 (Clontech) to generate pOMP<sup>6k</sup>:GFP and pOMP<sup>2k</sup>:GFP, respectively. To facilitate axonal localization of reporter protein, the *EGFP* cDNA of pOMP<sup>6k</sup>:GFP and pOMP<sup>2k</sup>:GFP was replaced with *EYFP-Mem* cDNA (Clontech), which encodes a fusion protein consisting of the N-terminal 20 amino acids of GAP-43 and EYFP. The resulting plasmids, pOMP<sup>6k</sup>:gap-YFP and pOMP<sup>2k</sup>:gap-YFP, were purified, linearized, and diluted to 50 ng/µl in distilled water containing 0.1% Phenol Red. The DNA solution was injected into the blastomere of one-cell stage embryos. Embryos with fluorescence were raised to sexual maturity and founder fish were identified by the expression of YFP-fluorescence in their progeny. Four transgenic lines were obtained from injections with pOMP<sup>6k</sup>:gap-YFP and pOMP<sup>2k</sup>:gap-YFP (two lines for each construct). Two lines, termed Tg(OMP<sup>6k</sup>:gap-YFP)<sup>rw031a</sup> and Tg(OMP<sup>2k</sup>:gap-YFP)<sup>rw032a</sup>, in which strong YFP fluorescence was observed, were used in this study.

### Fish lines

*astray* mutants (*ast*<sup>i272z</sup>) were kept as homozygotes because they are partially adult viable and fertile (Fricke et al., 2001). *ast* homozygotes

(*ast/ast*) were crossed with heterozygous Tg(OMP<sup>6k</sup>:gap-YFP)<sup>rw031a</sup> transgenic fish (abbreviated as *omp:yfp/+*), and then *ast/+;omp:yfp/+* fish were crossed with *ast* homozygotes to obtain *ast/ast;omp:yfp/+* embryos. To identify *ast/ast;omp:yfp/+* fish, genomic DNA was extracted from embryos, or fin-clips of adults, and typed by PCR amplification of a DNA fragment containing the *ast*<sup>i272z</sup> allele using the primers 5'-GAA TGA CTC CTC GTC GCT CT-3' and 5'-TAT GGT GGT AGG GCT AAG GAC-3', followed by direct sequencing of the PCR products. A transgenic line, Tg(*hsp70:Slit2-GFP*)<sup>rw015d</sup> (previously called HS2E-4S) (Yeo et al., 2001; Yeo et al., 2004), in which the Slit2-GFP fusion protein can be heat-induced, was used to overexpress Slit2.

### Whole-mount in situ hybridization

Digoxigenin (DIG)-labeled cRNA probes for *robo2* (Lee et al., 2001), *slit1a*, *slit1b* (Hutson et al., 2003), *slit2* and *slit3* (Yeo et al., 2001) were used. Whole-mount in situ hybridization was performed as previously described (Hauptmann and Gerster, 1994), with the following modifications. DIG-labeled probes synthesized by in vitro transcription were purified with Micro Bio-Spin 30 columns (Bio-Rad). Embryos were hybridized with probes overnight at 55°C in hybridization solution (2.5 mM EDTA, 300 mM NaCl, 50% formamide, 1 mg/ml yeast RNA, 1×Denhardt's solution, 5% dextran sulfate, 20 mM Tris-HCl at pH 8.0). After hybridization, embryos were treated with RNase A (20 µg/ml) for 30 minutes at 37°C.

### Dil-staining

Dil-staining of OSNs was carried out according to Dynes and Ngai (Dynes and Ngai, 1998).

### Immunohistochemistry

Whole-mount immunohistochemistry was carried out as previously described (Macdonald, 1999), with the following modifications. Embryos older than 2 days postfertilization (dpf) were fixed in 2% trichloroacetic acid in phosphate-buffered saline (PBS), and permeabilized in acetone for 7 minutes at -20°C. PBS containing 1% dimethylsulfoxide and 0.1% Tween-20 (PBBDT) was used as washing solution.

For simultaneous in situ detection of *robo2* transcripts and YFP antigens, immunostaining with diaminobenzidine was done first, as described above, except that MAB (100 mM maleic acid, 150 mM NaCl), containing 2% blocking reagent (Roche Diagnostics) and 0.5% heparin, was used for blocking and incubation solutions.

For immunostaining of adult OB sections, 12- to 14-month-old female fish (~4 cm body length) were anesthetized with 0.016% tricaine, and telencephalic hemispheres including OBs were dissected out. Tissues were fixed overnight at 4°C in 4% paraformaldehyde in PBS, equilibrated in 30% sucrose, frozen in O.C.T. Compound, sectioned on a cryostat (20 µm thickness), and mounted onto silane-coated glass slides. The sections were incubated sequentially with 5% NGS in PBS containing 0.1% Triton X-100, primary antibodies, and fluorescent dye-conjugated secondary antibodies.

Antibodies used were as follows: rabbit polyclonal anti-GFP antibody (1:1000, a kind gift from Dr N. Tamamaki); mouse monoclonal anti-calretinin antibody (1:1000, Swant); mouse monoclonal anti-SV2 antibody [1:20, supernatant, Developmental Studies Hybridoma Bank (DSHB) at University of Iowa]; mouse monoclonal *zns-2* antibody (1:200, supernatant, DSHB); rabbit polyclonal anti-PCAM antibody (rabbit IgG; 0.4 µg/ml); Alexa488-conjugated goat anti-rabbit IgG antibody (1:300, Molecular Probes); Cy3-conjugated goat anti-mouse IgG (1:300, Jackson ImmunoResearch); peroxidase-conjugated secondary antibody (Histofine Simple Stain Max PO, Nichirei, Tokyo, Japan). Anti-PCAM antiserum was produced by Sawaday Technology (Tokyo, Japan). A synthetic C-terminal peptide (20 amino acid residues) of zebrafish PCAM was conjugated with keyhole limpet hemocyanin, and a rabbit was immunized with the conjugate. The generated

antiserum was purified by immunoaffinity chromatography with peptide-coupled resin.

## Results

### Transient expression of *robo2* in the developing olfactory placode

We first conducted a detailed temporal expression analysis of *robo2* in the olfactory placode by whole-mount mRNA in situ hybridization, in order to shed light on its potential roles in olfactory axon guidance. In zebrafish, the olfactory placodes are first evident at 18–20 hpf between forebrain and eyes as thickenings of the ectoderm (Hansen and Zeiske, 1993). *robo2* expression in the olfactory placode could be detected at 20 hpf (Fig. 1B). From 24 to 36 hpf, when the early olfactory axons emerging from the olfactory placode grew toward the OB primordium, *robo2* mRNA was strongly expressed in the olfactory placode in addition to in the brain (Fig. 1C–E). At 48 hpf, when the pioneering olfactory axons had arrived at the OB primordium and started to form discrete axonal condensations (proto-glomeruli), *robo2* expression in the olfactory placode was greatly diminished and detectable only in a few cells located near the nasal pit, although its expression remained high in the brain (Fig. 1F). We were unable to detect evident *robo2* expression in adult OE by section in situ hybridization (data not shown).

### OSN axons make posterior pathfinding errors in *ast* embryos

To elucidate the role of *robo2* in the developing olfactory system, we examined the trajectories of OSN axons in *astray<sup>fl272z</sup>* (*ast*) mutant zebrafish, an allele that lacks a functional Robo2 receptor (Fricke et al., 2001). Because OSNs have dendrites whose cilia are exposed to the environment, we labeled OSNs by dipping the embryos into a solution containing DiI at 3.5 dpf (Dynes and Ngai, 1998). Following at least a 1-hour incubation to allow diffusion of DiI into axons, the trajectories of OSN axons were viewed from anterior and dorsal directions by confocal laser scanning microscopy. In wild type, OSN axons exited the OE through a restricted region on its medial side, forming a tightly fasciculated bundle (Fig. 2B). They extended dorsally soon after exiting the OE and then defasciculated tangentially on the surface of the OB (Fig. 2B,C). In *ast* homozygotes, many OSN axons reached the OB, but several axonal fibers misrouted posteriorly and penetrated into the diencephalon without reaching the OB (Fig. 2D–G). The posteriorly misrouting axons occasionally crossed the midline to the contralateral side (arrows in Fig. 2F,G). To assess phenotypic penetrance and strength, we counted the number of embryos having a given pathfinding error (Table 1). All *ast* homozygous embryos exhibited posterior pathfinding errors with some differences in maximal reach value, and ~50% of *ast* homozygotes had midline-crossing errors; such trajectories were never observed in wild-type or *ast* heterozygous embryos (Table 1).

### Dynamic axon behavior in *ast* embryos

Understanding how posterior pathfinding errors in *ast* embryos arise requires the visualization of dynamic axon behavior. For this purpose, we generated transgenic lines that express membrane-targeted YFP under the control of the zebrafish

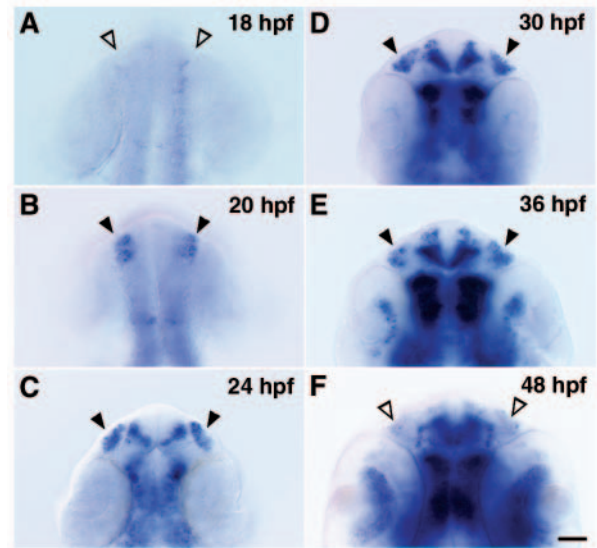


**Fig. 1.** Transient expression of *robo2* mRNA in the developing olfactory placode, shown by whole-mount in situ hybridization. (A–E) Dorsal views with anterior to the top; (F) ventral view with anterior to the top. As the olfactory placode moves from a dorsal to a more ventral location during development, it is more easily viewed from the ventral side at 48 hpf. Arrowheads (both open and closed) denote the position of the olfactory placode. *robo2* mRNA was detected in the olfactory placode in embryos at stages between 20–36 hpf (closed arrowheads in B–E). Scale bar: 50  $\mu$ m.

olfactory marker protein (OMP) promoter (Çelik et al., 2002; Yoshida et al., 2002). We then crossed *ast* to one of the transgenic lines, Tg(OMP<sup>6k</sup>:gap-YFP)<sup>rw031a</sup> (abbreviated as omp:yfp), and carried out time-lapse observation of dynamic OSN axon projections (Fig. 3). The zebrafish olfactory placode contains a transient population of neurons, which are morphologically and spatially distinct from OSNs: they are dendrite-less unipolar neurons whose cell bodies are situated in the ventromedial portion of the olfactory placode (Whitlock and Westerfield, 1998). At 1 dpf, YFP fluorescence was detected in ~10 unipolar neurons (closed arrowheads in Fig. 3A,F), and in several early developing OSNs with dendrites extending toward the presumptive olfactory pit (open arrowheads in Fig. 3A,F). Emergence of the axons from the olfactory placode was significantly retarded in *ast* homozygotes when compared with heterozygotes at 1 dpf (Fig. 3A,F). In *ast* homozygotes, many axons grew dorsally toward the OB primordium, but several axons misrouted ventromedially soon after exiting the olfactory placode at 1.5 dpf (short arrows in Fig. 3G). At 2 dpf, the axons that had misrouted at the exiting point formed fascicles and became prominent, with an increase in number of YFP-labeled OSNs (short arrows in Fig. 3H). By 3 dpf, the aberrant axonal fascicles had often penetrated the diencephalon, occasionally crossing the midline (Fig. 3I,J). At 3 dpf, the gross projections to OB were reduced in homozygotes when compared with heterozygotes (Fig. 3D,I). Notably, YFP-labeled dorsolateral glomeruli (thick arrows in Fig. 3D) disappeared in homozygotes (Fig. 3I). These observations demonstrate that the posteriorly projecting and midline-crossing errors arise in *ast* mutants at the time when the first olfactory axons leave the olfactory placode.

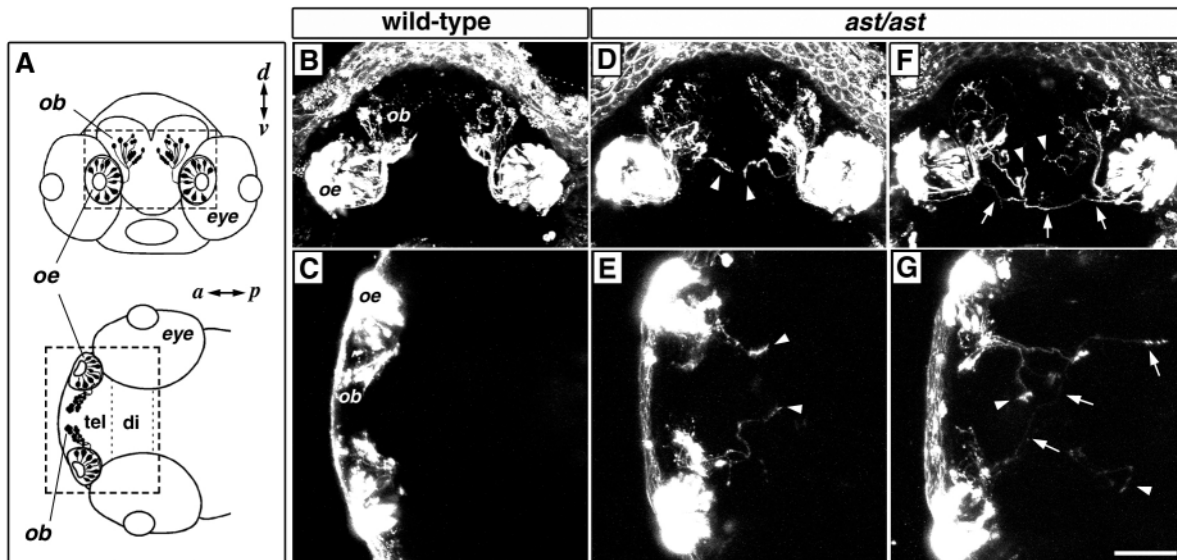


**Fig. 2.** *ast* embryos show OSN axon pathfinding defects. OSN axons in wild-type and homozygous *ast* embryos were labeled by external application of DiI at 3.5 days postfertilization (dpf) and viewed by confocal microscopy. (A) Diagrams representing frontal and dorsal views of the 3.5-dpf zebrafish head. ob, olfactory bulb; oe, olfactory epithelium; tel, telencephalon; di, diencephalon; a, anterior; p, posterior; d, dorsal; v, ventral. Broken rectangles indicate the region observed in B-G. (B-G) One wild-type (B,C) and two *ast* (D,E; F,G) examples are shown in frontal (B,D,F) and dorsal (C,E,G) views, as composite images generated from the series of optical sections. (D-G) In *ast* mutants, many axons reach the OB, but some fibers misroute posteriorly and penetrate into the diencephalon without reaching the OB (arrowheads and arrows). The posteriorly projecting fibers occasionally cross the midline (arrows in F,G). Scale bar: 100  $\mu$ m.

### The axons of unipolar neurons misroute in *ast* embryos

The earliest neurites emerging from the olfactory placode at 24 hpf have previously been identified as axons of the unipolar neurons (Whitlock and Westerfield, 1998; Whitlock and Westerfield, 2000). Thus, it is likely that the misrouting axons in *ast* embryos at the time when the first olfactory axons leave the olfactory placode are derived from the unipolar neurons. To clarify whether the unipolar neurons express *robo2*, we performed double in situ detection for *robo2* transcripts and YFP antigens in the *omp:yfp* transgenic line at 30 hpf. As described above, the unipolar neurons were readily distinguishable from OSNs by their unique location and morphology. Hybridization signals for *robo2* transcripts were uniformly distributed within the olfactory placode (Fig. 4A,B), and seen on the cell bodies of the unipolar neurons (arrowheads

in Fig. 4B), as well as in the early developing OSNs (arrows in Fig. 4B).

It has been reported that the *zns-2* antibody (Trevarrow et al., 1990) recognizes the axons of unipolar neurons (Whitlock and Westerfield, 1998). We therefore performed *zns-2*-labeling of 36-hpf *ast* embryos to assess whether or not the unipolar neurons make pathfinding errors in the absence of *Robo2* function. In wild type, the *zns-2*-positive axons formed a tight fascicle and extended dorsally along the surface of the telencephalon (Fig. 4C), whereas in *ast* mutants, the *zns-2*-positive axons defasciculated immediately after growing out of the olfactory placode and some of them misrouted ventromedially toward the midline (Fig. 4D). These trajectories resembled those of the early growing YFP-labeled axons observed in *ast/ast;omp:yfp/+* embryos (Fig. 3G). Because the dendrite-less unipolar neurons are unlabeled by external

**Table 1. Pathfinding defects of OSN axons in 3.5-dpf embryos**

	<i>n</i>	No obvious pathfinding errors	Posterior pathfinding errors			Midline-crossing errors
			Maximal reach* ( $\mu$ m)			
			<100	100-200	>200	
Wild type	13	13	0	0	0	0
<i>ast/+</i>	12	12	0	0	0	0
<i>ast/ast</i>	13	0	3	8	2	7
wt hs <sup>†</sup>	12	12	0	0	0	0
<i>slit2</i> no-hs <sup>‡</sup>	10	9	1	0	0	0
<i>slit2</i> hs <sup>§</sup>	12	0	2	9	1	8

OSN axons were labeled by external application of DiI at 3.5 dpf. Numbers indicate the number of embryos showing a given axon pathfinding error.

\*The distance from the boundary between the olfactory epithelium and the telencephalon to the farthest point of the posterior misrouted axons, measured from composite dorsal view images from a series of optical sections.

<sup>†</sup>Heat-induced wild-type embryos.

<sup>‡</sup>Non-heat-induced *hsp:slit2-gfp/+* embryos.

<sup>§</sup>Heat-induced *hsp:slit2-gfp/+* embryos.

application of DiI, the misrouting axons labeled by DiI in *ast* embryos should have originated from OSNs (Fig. 2D-G). Taken together, these results indicate that both unipolar neurons and OSNs make pathfinding errors in *ast* embryos.

### Spatial expression patterns of four members of Slit genes

To examine whether the *ast* phenotype correlates with the

expression of Slit genes, the Robo2 ligands, we conducted a detailed spatial expression analysis by whole-mount in situ hybridization (Fig. 5). All four members of the zebrafish Slit family, *slit1a*, *slit1b*, *slit2* and *slit3* (Yeo et al., 2001; Hutson et al., 2003) were expressed close to the olfactory axon trajectory during the initial phase of olfactory axon pathfinding. At 30 hpf, *slit1a*, *slit1b* and *slit2* were expressed in bilateral clusters of cells located near the boundary between the telencephalon and diencephalon (arrowheads in Fig. 5C,F,I). *slit1a* and *slit1b* were also expressed in bilateral clusters in the telencephalon (arrows in Fig. 5B,C,E,F), adjacent to the region where the pioneering olfactory axon termini were extending (Fig. 5N,O). *slit2* and *slit3* were expressed along the midline in the ventral forebrain (thick arrows in Fig. 5H,K). These regions of Slit expression were located posteriorly or ventromedially adjacent to the olfactory axon pathway (Fig. 5P), consistent with a function of Slits as chemorepellents for the Robo2-expressing olfactory axons. Such spatial expression patterns of Slit genes were maintained

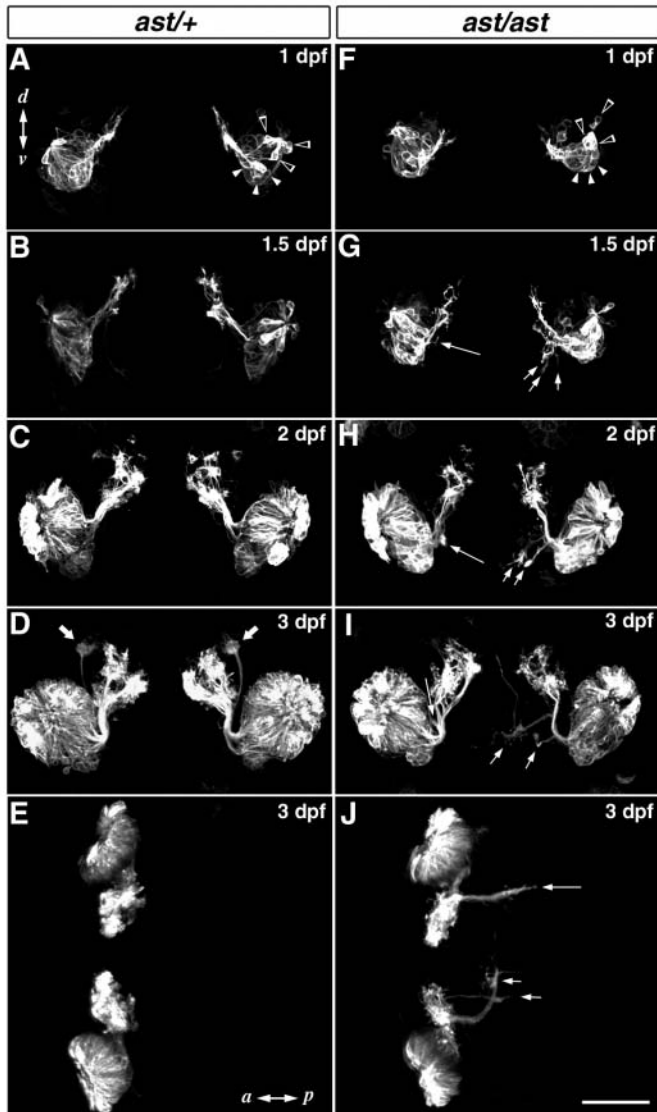


**Fig. 3.** Time-lapse observation of YFP-labeled olfactory axons in living embryos. Dynamic axon behaviors in representative *ast/+;omp:yfp/+* (A-E) and *ast/ast;omp:yfp/+* (F-J) embryos are shown. YFP expression under the control of the OMP promoter is observed in unipolar neurons (closed arrowheads in A,F), as well as in OSNs (open arrowheads in A,F). In the *ast* homozygote, several axons misroute ventromedially soon after exiting the olfactory placode at 1.5 dpf (short arrows in G). These misrouted axons form two fascicles at 2 dpf (short arrows in H), and further extend posteriorly to reach the diencephalon at 3 dpf (short arrows in I,J). A single aberrant fascicle that directly misprojects to the diencephalon is marked by the long arrows in G-J. Note that the YFP-labeled lateral glomeruli observed in the *ast* heterozygote (thick arrows in D) are not present in the homozygote (I). A-D,F-I, frontal views; E,J, dorsal views. Scale bar: 100  $\mu$ m.

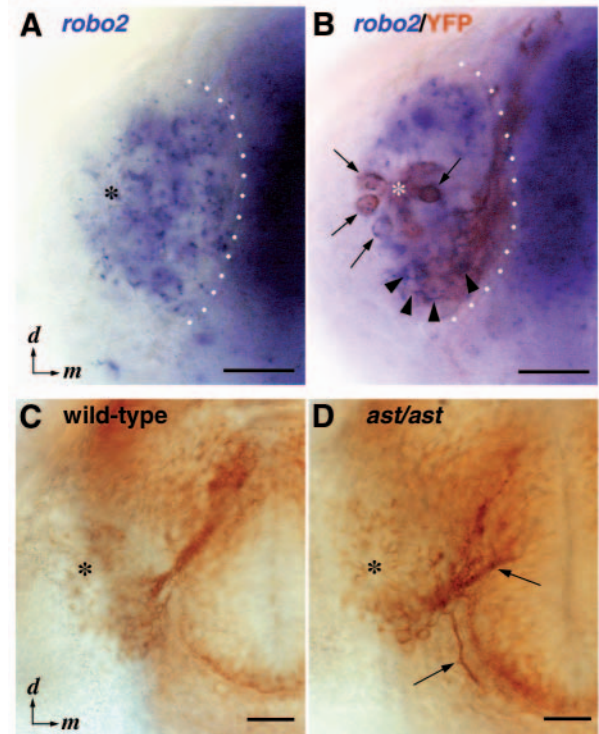


**Fig. 4.** The unipolar neurons express *robo2* and make pathfinding errors in *ast* embryos. (A,B) Frontal views of the olfactory placode of 30-hpf *omp:yfp/+* embryos. (A) Whole-mount in situ hybridization. Blue dots are signals for *robo2* mRNA on the focal plane. Broad blue staining in the olfactory placode is derived from signals on cells that are out of the focal plane. (B) Double staining for *robo2* mRNA and YFP antigen. Early developing OSNs (arrows) and unipolar neurons (arrowheads) are stained in brown with anti-GFP antibody. Hybridization signals for *robo2* mRNA (blue dots) are seen on the somata of both cell types. White dotted lines indicate the boundary between the olfactory placode and telencephalon. (C,D) Frontal views of the head of wild-type (C) and *ast* homozygous (D) embryos stained with *zns-2* antibody at 36 hpf. The *zns-2*-positive axons misroute medially or ventromedially immediately after exiting the olfactory placode in *ast* embryos (arrows in D). Asterisks mark the position of the olfactory pit. d, dorsal; m, medial. Scale bar: 50  $\mu$ m.

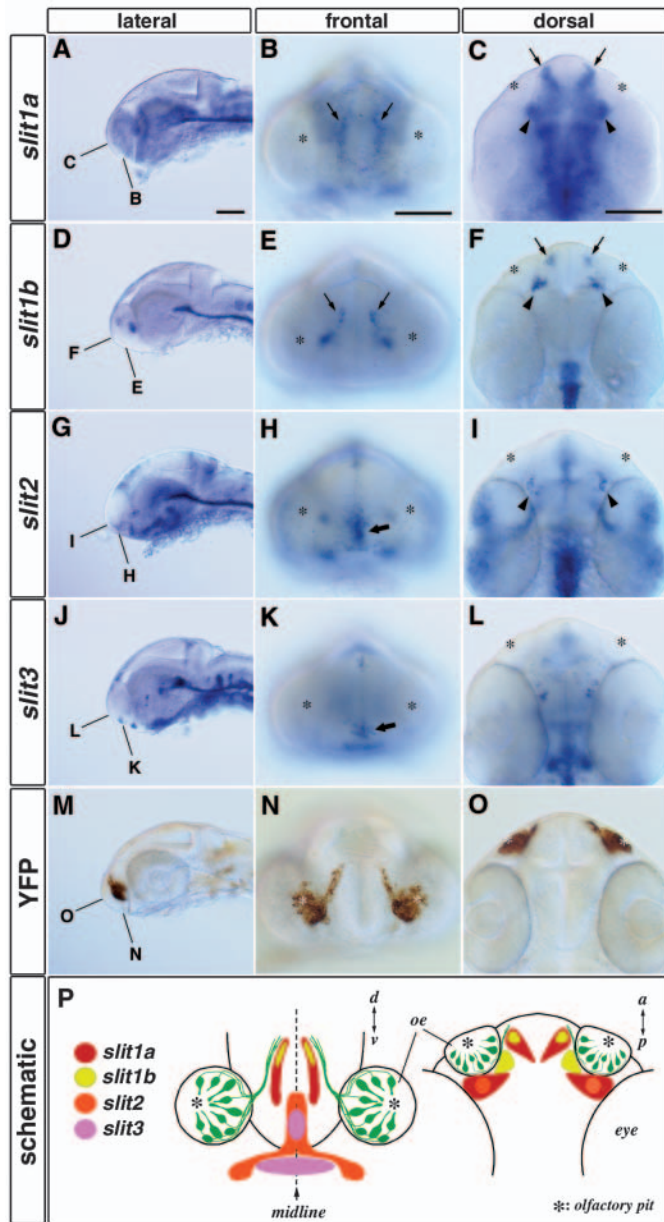


**Fig. 5.** Spatial expression patterns of four Slit mRNAs are consistent with a function as repulsive cues for the olfactory axons. Heads of 30-hpf whole-mounted embryos hybridized with *slit1a* (A-C), *slit1b* (D-F), *slit2* (G-I) and *slit3* (J-L) probes. The olfactory axon trajectory of a Tg(*OMP<sup>2k</sup>:gap-YFP*)<sup>rw032a</sup> transgenic embryo stained with anti-GFP antibody is shown in M-O. *slit1a*, *slit1b* and *slit2* are expressed in bilateral clusters of cells located near the boundary between the telencephalon and diencephalon (arrowheads in C,F,I). *slit1a* and *slit1b* are also expressed bilaterally in the telencephalon (arrows in B,C,E,F). *slit2* and *slit3* are expressed along the midline in the ventral forebrain (thick arrows in H,K). The correlation between the regions of Slit expression and the olfactory axon trajectory (green) is schematized in P. A,D,G,J,M, lateral views with anterior to the left; B,E,H,K,N, frontal views with dorsal to the top; C,F,I,L,O, dorsal views with anterior to the top. The focal planes of frontal (B,E,H,K,N) and dorsal (C,F,I,L,O) views are indicated in the corresponding leftmost panels (A,D,G,J,M). Asterisks mark the position of the olfactory pit. Scale bar: 100  $\mu$ m.

from 24 to 36 hpf (data not shown). These results suggest that the *ast* phenotype may be attributed to a defect in Robo2/Slit signaling that normally prevents olfactory axons from entering into inappropriate areas.

### Ubiquitous misexpression of Slit2 impairs OSN axon pathfinding

We previously demonstrated that ubiquitous overexpression of Slit2 in transgenic zebrafish causes pathfinding errors of the axons of Mauthner neurons and the central axons of trigeminal sensory ganglion neurons (Yeo et al., 2004). We therefore investigated whether localized Slit sources are critical for OSN axon pathfinding, by inducing ubiquitous misexpression of Slit. We used a transgenic line, Tg(*hsp70:Slit2-GFP*)<sup>rw015d</sup> (abbreviated as *hsp:slit2-gfp*), in which a Slit2-GFP fusion protein could be induced ubiquitously following an increase in ambient temperature (to 39°C for 50 minutes) (Yeo et al., 2001; Yeo et al., 2004). Heterozygous *hsp:slit2-gfp* embryos were heat-induced at 19 hpf and re-induced at 31 hpf to maintain the Slit2 expression level during the period of initial olfactory axon outgrowth. At 3.5 dpf, OSN axons in the heat-induced *hsp:slit2-gfp* transgenic embryos were labeled by external application of DiI and the trajectories were analyzed by confocal microscopy. Intriguingly, the resulting phenotype of Slit2-overexpressing embryos resembled the Robo2 loss-of-function phenotype: some axonal fibers misrouted posteriorly and penetrated into the diencephalon, occasionally crossing the midline (Fig. 6). The phenotypic penetrance and strength were also similar to *ast* homozygous mutants (Table 1). It is likely that when Slit2 is ubiquitously expressed, the olfactory axons are impaired in their ability to respond to the local repulsive cues of endogenous Slit proteins. These results suggest that olfactory axons can indeed respond to Slit, and that the precise patterns of Slit expression are critical for navigation of OSN axons to the OB.

### Defasciculation of the olfactory nerve and impaired formation of proto-glomeruli in *ast* embryos

In *ast* mutants, even in the embryos with the strongest phenotype, the majority of axons can reach the OB. To further evaluate the effects of loss of Robo2 function in development of the primary olfactory pathway, we carried out whole-mount immunohistochemical analysis of 72-hpf *ast* embryos with antibodies that reveal the integrity of the olfactory nerve and proto-glomerular organization. An antibody against PCAM, a zebrafish NCAM-related cell adhesion molecule (Mizuno et al., 2001), labeled all OSN axon shafts and termini, with no staining of cell bodies (Fig. 7A). In wild type, olfactory axons were tightly fasciculated to form a single bundle until they entered the OB (brackets in Fig. 7A,C). By contrast, we found in *ast* embryos that olfactory axons were defasciculated before reaching the OB (brackets in Fig. 7D,F) and some small axon bundles entered the OB from improper entry sites (arrows in Fig. 7D,F). PCAM immunoreactivity of axon termini was somewhat weaker in *ast* mutants than in wild type (Fig. 7A,D,G,J). The proto-glomeruli immunostained for SV2, a synaptic vesicle protein, in *ast* embryos were irregular in shape and were less clearly defined than those in wild type (Fig. 7H,I,K,L). Anti-calretinin antibody labeled cell bodies of a small subpopulation of OSNs and their target proto-glomeruli (Fig. 7B). The majority of calretinin-positive axons projected

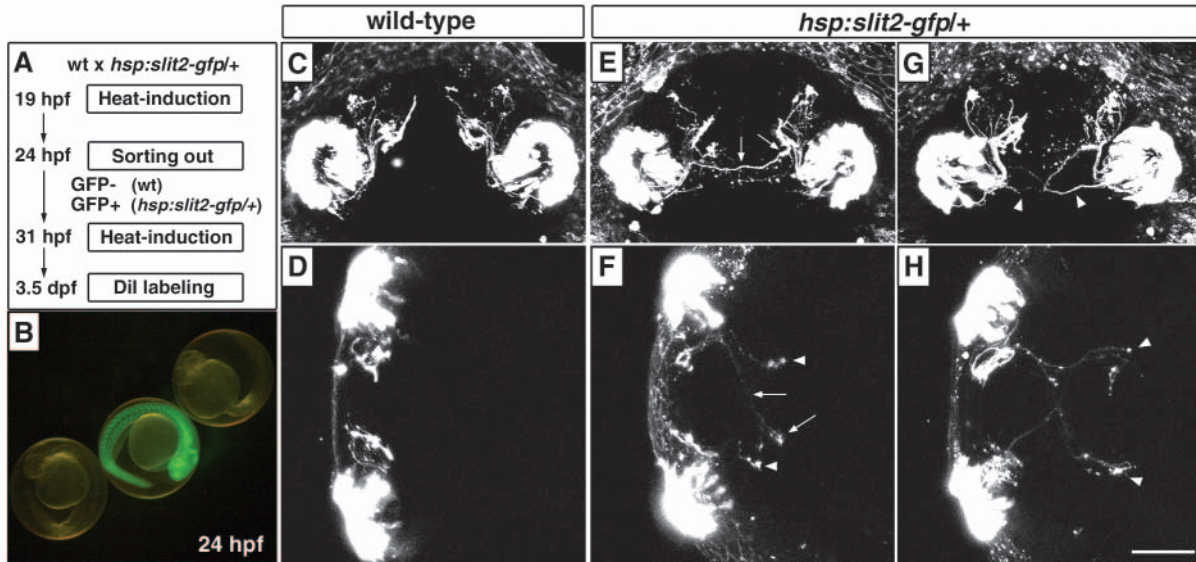


**Fig. 6.** Ubiquitous misexpression of Slit2 causes posterior pathfinding errors of OSN axons. (A) Schematic of the experimental procedure. (B) A heterozygous *hsp:slit2-gfp* transgenic embryo overexpressing a Slit2-GFP fusion protein (green) and wild-type siblings at 24 hpf, which had received heat-shock treatment at 19 hpf. (C-H) One wild-type and two *hsp:slit2-gfp/+* examples are shown. In Slit2-overexpressing embryos, some axonal fibers are deviated from the normal pathway and extend posteriorly (arrowheads and arrows in E-H), occasionally crossing the midline (arrows in E,F). C,E,G, frontal views with dorsal to the top; D,F,H, dorsal views with anterior to the left. Scale bar: 100  $\mu$ m.

laterally to form two discrete proto-glomeruli in wild type (thick arrows in Fig. 7B,C), whereas in *ast* mutants, only one irregularly shaped proto-glomerulus was seen at the lateralmost position of the OB (thick arrows in Fig. 7E,F). This aberrant calretinin-positive proto-glomerulus in *ast* mutants was somewhat larger in size than the normal calretinin-positive proto-glomerulus seen in wild type, implying the loss of proper segregation of these proto-glomeruli in *ast* mutants. These results demonstrate that Robo2 function is necessary for maintaining the integrity of the olfactory nerve and proto-glomerular organization.

#### ***ast* adults show disorganized glomerular map of OB**

We found that a specific subpopulation of OSNs projecting their axons mainly to the dorsal and medial portion of the OB express YFP under the control of zebrafish OMP promoter (Fig. 3D; Fig. 8A) (Y.S., N.M. and Y.Y., unpublished), although this had not been described in the previous studies using the OMP promoter (Çelik et al., 2002; Yoshida et al., 2002). As the projection patterns of YFP-labeled axons were essentially the same in the four independent lines generated (data not shown), the restriction of expression to a subpopulation of OSNs is probably not due to a positional effect of the transgene integration sites. To elucidate whether the loss of Robo2 function affects the topographic glomerular map of the OB in adult fish, we examined the spatial arrangement of glomeruli innervated by YFP-labeled axons in *ast/ast;omp:yfp/+* adults. OBs of *ast* adults [dorsal-to-ventral (D-V) thickness,  $460 \pm 10$   $\mu$ m; anterior-to-posterior (A-P) length,  $458 \pm 9$   $\mu$ m; medial-to-lateral (M-L) width,  $458 \pm 4$   $\mu$ m;  $n=5$ , mean  $\pm$  s.e.m.] were slightly smaller in size than those of wild-type adults (D-V,  $508 \pm 6$   $\mu$ m; A-P,  $492 \pm 8$   $\mu$ m; M-L,  $442 \pm 6$   $\mu$ m;  $n=5$ ; Fig. 8A-D). Whole-mount observation of OBs revealed that in *ast* mutants, dorsally projecting YFP-labeled fibers were reduced in number, whereas the intensity of YFP

fluorescence in the ventral portion of the OB was increased (Fig. 8A,C). Notably, the posterolaterally located YFP-labeled glomeruli observed in wild type (arrowheads in Fig. 8A) were not observed in *ast* adults (Fig. 8C), whereas ectopic glomerulus-like structures were found in the posteroventral portion of the OB (arrows in Fig. 8C). A similar projection pattern was observed in all individual *ast* adults ( $n=6$ ). We also found that only one *ast* adult exhibited a posterior misprojection outside of the OB (Fig. 8E,F), although all *ast* embryos showed posterior pathfinding errors at 3.5 dpf (Table 1). This implies the retraction or elimination of the posteriorly misrouted axons during maturation, so that the ectopic glomerulus-like structures seen in the posteroventral portion of OB (arrows in Fig. 8C) might be formed by the retracted axons. To analyze the spatial arrangement of glomeruli in more detail, we carried out immunohistochemical staining of OB sagittal sections (Fig. 8B,D). The sections were counterstained with an anti-SV2 antibody to distinguish the glomerular layer from the olfactory nerve layer. In *ast* mutants, YFP-labeled axons ectopically innervated anteroventral and posteroventral glomeruli (arrows in Fig. 8D). In addition, aberrant axonal fascicles penetrated deep into the cellular layer of the OB (arrowheads in Fig. 8D) and eventually formed glomeruli in the posterodorsal region. Thus, glomerular organization of the OB is perturbed in *ast* adults despite the fact that *robo2* expression in the OE is restricted to embryos at stages between 20 and 36 hpf (Fig. 1). These results suggest an importance of early olfactory axon guidance in determining a topographic glomerular map in the adult OB.

#### **Discussion**

We show that Robo2/Slit signaling controls navigation of the early growing olfactory axons toward the OB primordium. Furthermore, we demonstrate that the spatial arrangement of

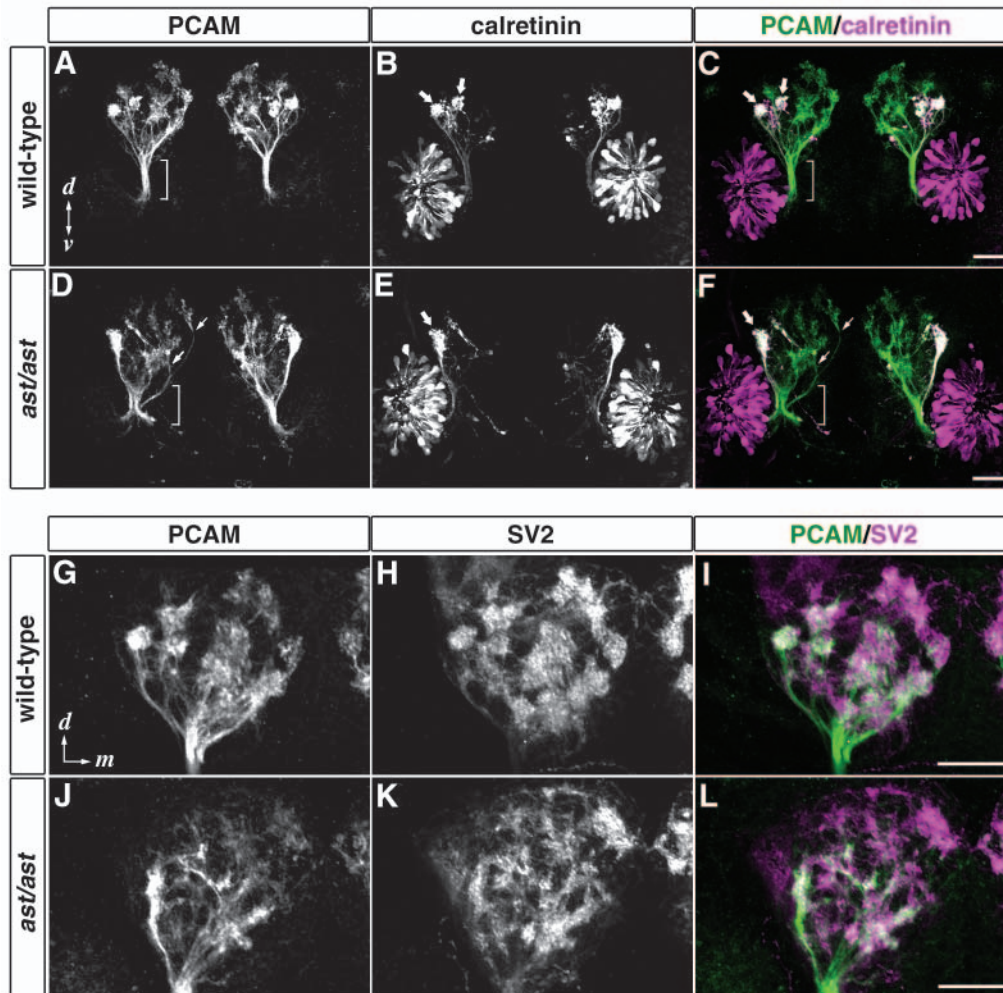


**Fig. 7.** *ast* embryos show defasciculation of the olfactory nerve and impaired proto-glomerular organization. Frontal views of the head of wild-type (A-C,G-I) and *ast* homozygous (D-F,J-L) 72-hpf embryos stained with antibodies against PCAM (A,D,G,I; green in C,F,I,L), calretinin (B,E; magenta in C,F) and SV2 (H,K; magenta in I,L). (A-F) In wild type, olfactory axons maintain a tightly fasciculated state until they enter the OB (brackets in A,C). By contrast, olfactory axons in *ast* are defasciculated before reaching the OB (brackets in D,F) and some fibers enter the OB from improper entry sites (arrows in D,F). Calretinin-positive axons mainly project laterally to form two discrete proto-glomeruli in wild type (thick arrows in B,C), whereas in *ast*, only one irregularly shaped proto-glomerulus is seen at the lateralmost position in the OB (thick arrows in E,F). (G-L) Proto-glomeruli stained with antibodies against PCAM and SV2 in *ast* embryos (J-L) are less clearly defined than those in wild type (G-I). d, dorsal; v, ventral; m, medial. Scale bar: 50  $\mu$ m.

glomeruli in the adult OB is perturbed by loss of Robo2 function. These results support the notion that the initial axonal scaffold established during embryogenesis is essential for determining a topographic glomerular map.

### Robo2 steers early olfactory axons toward the OB primordium

Whitlock and Westerfield reported that the initial connections between the olfactory placode and the OB primordium were provided by the axons of a transient population of unipolar neurons, which they called 'pioneer' neurons (Whitlock and Westerfield, 1998). *robo2* is transiently expressed in the olfactory placode and its temporal expression parallels the axon outgrowth of unipolar neurons (Fig. 1). Moreover, the unipolar neurons express *robo2* and make pathfinding errors without Robo2 function (Fig. 4). These results suggest that Robo2-mediated signaling directly regulates the axon pathfinding of the unipolar neurons.

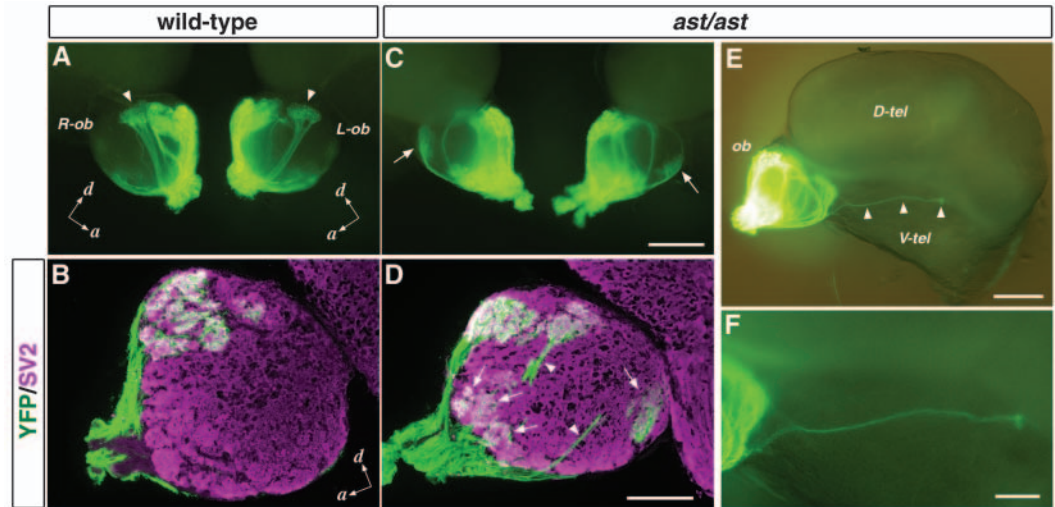
OSN axons also make pathfinding errors in *ast* embryos. Similar to the unipolar neurons, Robo2 may directly regulate the axon pathfinding of early developing OSNs, because these neurons also express *robo2* (Fig. 4). Alternatively, the axons of OSNs may make pathfinding errors non-autonomously by following the misrouted axons of the presumptive 'pioneer' unipolar neurons in *ast* mutants. It has been reported that

ablation of the unipolar neurons results in misrouting of the following OSN axons (Whitlock and Westerfield, 1998), suggesting that the unipolar neurons provide an essential scaffold for subsequently projecting OSN axons. In the absence of the unipolar neurons, the misrouted OSN axons typically extend posteriorly toward the diencephalon (Whitlock and Westerfield, 1998), resembling the trajectory in *ast* embryos observed in this study (Fig. 2). Further experiments, such as inhibition of Robo2 function selectively in the unipolar neurons, will clarify whether or not the OSN axons make pathfinding errors cell-autonomously.

### Slit proteins act as surround repulsive cues for olfactory axons

The summed region of Slit expression and the trajectory of *robo2*-expressing early olfactory axons are situated in a complementary manner, consistent with a function of Slit proteins as chemorepulsive ligands for Robo2. The spatial expression patterns of Slit genes could explain how the pathfinding errors observed in *ast* are normally prevented. *slit1a*, *slit1b* and *slit2* expressed near the telencephalon/diencephalon boundary (arrowheads in Fig. 5C,F,I) could function as a barrier to prevent olfactory axons from entering into the diencephalon. *slit2* and *slit3* along the midline in the ventral forebrain (thick arrows in Fig. 5H,K) could act to

**Fig. 8.** *ast* adults exhibit a disorganized glomerular map of the OB. The projection pattern of a subpopulation of OSNs was visualized by the OMP promoter-directed YFP expression in *omp:yfp/+* and *ast/ast;omp:yfp/+* adults. (A,C) Whole-mount lateral views of OBs under a fluorescence stereomicroscope. Note that the posterolaterally located glomeruli observed in wild type (arrowheads in A) are not present in *ast* mutants (C), whereas ectopic glomerulus-like structures are seen in the posteroventral portion of the OB in *ast* mutants (arrows in C).



(B,D) Double immunostaining with antibodies against YFP (green) and SV2 (magenta) of sagittal sections through the entrance point of the olfactory nerve at the anterior tip of OB. YFP-labeled axons ectopically innervate anteroventral and posteroventral glomeruli in *ast* mutants (arrows in D). In addition, aberrant axonal fascicles penetrate through the cellular layer of the OB (arrowheads in D). (E) Whole-mount lateral view of the left telencephalic hemisphere in an *ast* adult. A single fluorescent fascicle passes through the posteroventral surface of the OB and penetrates into the ventral telencephalic area (arrowheads). (F) Higher magnification view of the misprojecting fascicle shown in E. ob, olfactory bulb; R, right; L, left; D-tel, dorsal telencephalon; V-tel, ventral telencephalon; a, anterior; d, dorsal. Scale bar: in C, 250  $\mu$ m for A,C; in D, 100  $\mu$ m for B,D; in E, 250  $\mu$ m; in F, 100  $\mu$ m.

promote dorsally directed outgrowth and to prevent midline-crossing. Telencephalic *slit1a* and *slit1b* (arrows in Fig. 5B,C,E,F) could play a role in limiting the extension of olfactory axons on the surface of the OB. Thus, the spatial expression patterns of Slit genes support a 'surround repulsion' model, in which chemorepulsive cues produced by surrounding tissues channel axons into a specific route (Keynes et al., 1997).

We demonstrate that ubiquitous misexpression of Slit2 causes OSN axon pathfinding errors resembling the *ast* phenotype. It is surprising that the OSN axons do not simply retract or stall. However, a similar situation was observed following Slit2 overexpression with Mauthner axons (Yeo et al., 2004) and retinal axons (L.D.H. and C.-B.C., unpublished). Mauthner axons aberrantly re-cross the midline and retinal axons display an *ast*-like phenotype. Moreover, when Slit is pan-neurally expressed throughout the CNS of *Drosophila*, commissural axons exhibit an abnormality resembling the loss-of-function phenotype of Robo (Kidd et al., 1999). In all cases, ubiquitous Slit overexpression does not prevent axon outgrowth, but causes axon misrouting. Such phenotypes of Slit overexpression could be explained by a hypothetical 'gradient reading' model in which axonal growth cones would change their direction by reading a concentration gradient of a guidance cue (Walter et al., 1990). In this model, the repulsive cue does not influence the axonal outgrowth activity of neurons. Therefore, even if the gradient of Slit were lost by forced ubiquitous expression of Slit2, the OSN axons would not stall, and would grow well on a uniform field of the repulsive cue. However, an alternative possibility cannot be excluded: the OSN growth cones habituate and lose sensitivity to Slit by the continuous exposure of a high concentration of exogenous Slit2. In either case, the phenotype of Slit2 overexpression strongly suggests that OSN axons are responsive to Slit secreted from local sources and that the

precise patterns of Slit expression are crucial for OSN axon pathfinding.

Although Robo2/Slit signaling is important for the proper navigation of the nascent olfactory axons toward the OB primordium, other guidance mechanisms must be involved in this process, as evidenced by the fact that many olfactory axons can reach the OB primordium in *ast* embryos (Fig. 3). In rodents, cell adhesion molecules, such as L1 and NCAM, have been implicated in the initial assembly of olfactory pathway (Gong and Shipley, 1996; Whitesides and LaMantia, 1996). In zebrafish, L1 (Tongiorgi et al., 1995), NCAM and its related molecule PCAM (N.M. and Y.Y., unpublished) are also expressed in the olfactory placode at the time of initial axon outgrowth, and are thus candidate molecules functioning in concert with Robo2. Netrins act as attractive cues via transmembrane receptors of the DCC subgroup of Ig superfamily (Chisholm and Tessier-Lavigne, 1999). In rat, Netrin 1 expression is associated with DCC-positive olfactory axons only during the period of initial olfactory axon outgrowth (Astic et al., 2002), suggesting that Netrin 1 may play a role in promoting outgrowth of the nascent olfactory axons toward the OB primordium. Thus, it is likely that the combinatorial actions of attractive and repulsive cues mediate the proper navigation of the early growing olfactory axons.

### Robo2 is required for maintaining integrity of the olfactory nerve and proto-glomerular organization

Analysis of the olfactory nerve in 72-hpf *ast* embryos revealed that Robo2 is required to maintain olfactory axons in a tightly fasciculated state until they reach the developing OB. A feasible mechanism is that secreted Slit proteins near the olfactory nerve act to maintain axons within the main bundle through surround repulsion. Alternatively, a Slit-independent mechanism may be involved in fasciculation of the olfactory nerve, because the fasciculation defect in Slit2-overexpressing

embryos is somewhat less severe than that in *ast* mutants (data not shown). Homophilic and heterophilic interactions of cell adhesion molecules are thought to be important for axonal fasciculation. A recent *in vitro* study has shown that human Robo1 and Robo2 exhibit homophilic binding activity, as do the Ig superfamily adhesion molecules (Hivert et al., 2002). Thus, Robo2 may regulate the adhesive property of olfactory axons via a homophilic binding mechanism *in vivo*.

A bilateral symmetric and stereotyped arrangement of proto-glomeruli in the developing OB becomes evident between 48 and 72 hpf, after *robo2* expression in the olfactory placode has been downregulated. The proto-glomerular organization is impaired in *ast* embryos at 72 hpf, as revealed by staining with antibodies against SV2, PCAM and calretinin (Fig. 7). The precise mechanism that could explain such defects in *ast* embryos is unclear. One possibility is that a tightly fasciculated state of the olfactory nerve before reaching the developing OB could be crucial for the subsequent formation of proto-glomeruli. Aberrant defasciculation of the olfactory nerve in *ast* embryos results in the entrance of some fibers into OB from improper positions (arrows in Fig. 7D-F). These axons could encounter an inappropriate environment of putative guidance cues within the developing OB, leading to abnormal axonal sorting and impaired proto-glomerular formation. Alternatively, Robo2 expressed in the developing OB (Fig. 1) may contribute to dendritic morphogenesis of OB neurons and formation of proto-glomeruli, because Robo/Slit signaling has been shown to regulate dendritic development of cortical pyramidal neurons in rodents (Whitford et al., 2002). Selective removal of Robo2 function in the peripheral olfactory neurons or the OB neurons will be necessary to distinguish these possibilities.

### Impaired glomerular map in adult *ast* OB

*ast* adults exhibit impaired spatial arrangement of glomeruli in the OB (Fig. 8). Robo/Slit signaling has recently been implicated in topographic axonal projections in the *Drosophila* olfactory system (Jhaveri et al., 2004) and in the mouse vomeronasal system (Knöll et al., 2003; Cloutier et al., 2004). In *Drosophila*, different populations of OSNs express distinct combinations of Robos, and perturbation of Robo levels by loss of function or ectopic expression causes aberrant positioning of OSN axon termini in the antennal lobe. In mouse, Robo2 is expressed by the axons of vomeronasal sensory neurons located in the basal zone of the vomeronasal organ (VNO), whereas Slit1 and Slit3 are expressed in the accessory olfactory bulb (AOB), with a higher concentration in the anterior region where the axons from basal VNO do not project (Knöll et al., 2003). *slit1*-deficient mice exhibit ectopic innervation of anterior AOB by the axons from basal VNO (Cloutier et al., 2004). In both cases (fly and mouse), Robos are expressed in peripheral sensory neurons throughout the period when the topographic axonal projection is established.

By contrast, the expression of zebrafish *robo2* in peripheral olfactory neurons is restricted between 20 and 36 hpf (Fig. 1). Thus, Robo2 function in OSNs should be limited to the initial phase of olfactory axon pathfinding. We found that *ast* adults exhibit abnormal innervation of ventral glomeruli by YFP-labeled axons, concomitant with the reduction of dorsally projecting fibers, despite the continual renewal of OSNs

throughout life. This finding raises a possibility that later developing OSNs project their axons to target glomeruli using the pre-existing fibers as a scaffold. Removal of Robo2 function causes ventromedial and posterior pathfinding errors of early growing olfactory axons (Figs 2, 3), probably due to the loss of sensitivity to Slit2/Slit3 and Slit1a/Slit1b expressed ventromedially and posteriorly adjacent to the OB primordium, respectively (Fig. 5). Later developing OSN axons would follow the trajectory of early misrouting axons, resulting in the ectopic innervation of ventral glomeruli and thus the maintenance of an aberrant topographic map in adult. However, it also seems possible that later OSN axons do not rely on any pre-existing fibers for pathfinding, but rather depend on their targets, as the formation of proto-glomeruli is impaired in *ast* embryos (Fig. 7). Further experiments will be required to verify these possibilities.

In conclusion, Robo2/Slit signaling guides early growing olfactory axons toward the OB primordium and is required for constructing a precise glomerular map in the adult OB.

We thank Toshio Miyashita (RIKEN BSI) for continual advice on this research; Osamu Uemura (RIKEN BSI) for technical advice on the generation of transgenic zebrafish; and Nobuaki Tamamaki (Kumamoto University) for the gift of the rabbit anti-GFP antibody. We also thank members of the Yoshihara and Okamoto laboratories for helpful discussions. This work was supported in part by: a Grant-in-Aid for Young Scientists to N.M. and a Grant-in-Aid for Scientific Research on Priority Area (C) – Advanced Brain Science Project – to Y.Y. from the Ministry of Education, Culture, Sports, Science, and Technology of Japan; by Special Coordination Funds for Promoting Science and Technology to Y.Y. from Japan Science and Technology Corporation (JST); and by NIH grant R01 EY12873 to C.-B.C.

### References

- Astic, L., Pellier-Monnin, V., Saucier, D., Charrier, C. and Mehlen, P. (2002). Expression of netrin-1 and netrin-1 receptor, DCC, in the rat olfactory nerve pathway during development and axonal regeneration. *Neuroscience* **109**, 643-656.
- Bagri, A., Marin, O., Plump, A. S., Mak, J., Pleasure, S. J., Rubenstein, J. L. and Tessier-Lavigne, M. (2002). Slit proteins prevent midline crossing and determine the dorsoventral position of major axonal pathways in the mammalian forebrain. *Neuron* **33**, 233-248.
- Çelik, A., Fuss, S. H. and Korsching, S. I. (2002). Selective targeting of zebrafish olfactory receptor neurons by the endogenous OMP promoter. *Eur. J. Neurosci.* **15**, 798-806.
- Chisholm, A. and Tessier-Lavigne, M. (1999). Conservation and divergence of axon guidance mechanisms. *Curr. Opin. Neurobiol.* **9**, 603-615.
- Cloutier, J. F., Sahay, A., Chang, E. C., Tessier-Lavigne, M., Dulac, C., Kolodkin, A. L. and Ginty, D. D. (2004). Differential requirements for semaphorin 3F and Slit-1 in axonal targeting, fasciculation, and segregation of olfactory sensory neuron projections. *J. Neurosci.* **24**, 9087-9096.
- Cutforth, T., Moring, L., Mendelsohn, M., Nemes, A., Shah, N. M., Kim, M. M., Frisen, J. and Axel, R. (2003). Axonal ephrin-As and odorant receptors: coordinate determination of the olfactory sensory map. *Cell* **114**, 311-322.
- Dynes, J. L. and Ngai, J. (1998). Pathfinding of olfactory neuron axons to stereotyped glomerular targets revealed by dynamic imaging in living zebrafish embryos. *Neuron* **20**, 1081-1091.
- Feinstein, P. and Mombaerts, P. (2004). A contextual model for axonal sorting into glomeruli in the mouse olfactory system. *Cell* **117**, 817-831.
- Feinstein, P., Bozza, T., Rodriguez, I., Vassalli, A. and Mombaerts, P. (2004). Axon guidance of mouse olfactory sensory neurons by odorant receptors and the beta2 adrenergic receptor. *Cell* **117**, 833-846.
- Fricke, C., Lee, J. S., Geiger-Rudolph, S., Bonhoeffer, F. and Chien, C. B. (2001). *astray*, a zebrafish roundabout homolog required for retinal axon guidance. *Science* **292**, 507-510.
- Gong, Q. and Shipley, M. T. (1996). Expression of extracellular matrix

- molecules and cell surface molecules in the olfactory nerve pathway during early development. *J. Comp. Neurol.* **366**, 1-14.
- Hansen, A. and Zeiske, E.** (1993). Development of the olfactory organ in the zebrafish, *Brachydanio rerio*. *J. Comp. Neurol.* **333**, 289-300.
- Hauptmann, G. and Gerster, T.** (1994). Two-color whole-mount in situ hybridization to vertebrate and *Drosophila* embryos. *Trends Genet.* **10**, 266.
- Hivert, B., Liu, Z., Chuang, C. Y., Doherty, P. and Sundaresan, V.** (2002). Robo1 and Robo2 are homophilic binding molecules that promote axonal growth. *Mol. Cell. Neurosci.* **21**, 534-545.
- Hutson, L. D. and Chien, C. B.** (2002). Pathfinding and error correction by retinal axons: the role of *astray/robo2*. *Neuron* **33**, 205-217.
- Hutson, L. D., Jurynech, M. J., Yeo, S. Y., Okamoto, H. and Chien, C. B.** (2003). Two divergent slit1 genes in zebrafish. *Dev. Dyn.* **228**, 358-369.
- Jhaveri, D., Saharan, S., Sen, A. and Rodrigues, V.** (2004). Positioning sensory terminals in the olfactory lobe of *Drosophila* by Robo signaling. *Development* **131**, 1903-1912.
- Keynes, R., Tannahill, D., Morgenstern, D. A., Johnson, A. R., Cook, G. M. and Pini, A.** (1997). Surround repulsion of spinal sensory axons in higher vertebrate embryos. *Neuron* **18**, 889-897.
- Kidd, T., Brose, K., Mitchell, K. J., Fetter, R. D., Tessier-Lavigne, M., Goodman, C. S. and Tear, G.** (1998). Roundabout controls axon crossing of the CNS midline and defines a novel subfamily of evolutionarily conserved guidance receptors. *Cell* **92**, 205-215.
- Kidd, T., Bland, K. S. and Goodman, C. S.** (1999). Slit is the midline repellent for the robo receptor in *Drosophila*. *Cell* **96**, 785-794.
- Kimmel, C. B., Ballard, W. W., Kimmel, S. R., Ullmann, B. and Schilling, T. F.** (1995). Stages of embryonic development of the zebrafish. *Dev. Dyn.* **203**, 253-310.
- Knöll, B., Schmidt, H., Andrews, W., Guthrie, S., Pini, A., Sundaresan, V. and Drescher, U.** (2003). On the topographic targeting of basal vomeronasal axons through Slit-mediated chemorepulsion. *Development* **130**, 5073-5082.
- Lee, J. S., Ray, R. and Chien, C. B.** (2001). Cloning and expression of three zebrafish roundabout homologs suggest roles in axon guidance and cell migration. *Dev. Dyn.* **221**, 216-230.
- Long, H., Sabatier, C., Ma, L., Plump, A., Yuan, W., Ornitz, D. M., Tamada, A., Murakami, F., Goodman, C. S. and Tessier-Lavigne, M.** (2004). Conserved roles for Slit and Robo proteins in midline commissural axon guidance. *Neuron* **42**, 213-223.
- Macdonald, R.** (1999). Zebrafish immunohistochemistry. In *Molecular Methods in Developmental Biology: Xenopus and Zebrafish* (ed. M. Guille), pp. 77-88. New Jersey: Humana Press.
- Marillat, V., Cases, O., Nguyen-Ba-Charvet, K. T., Tessier-Lavigne, M., Sotelo, C. and Chédotal, A.** (2002). Spatiotemporal expression patterns of slit and robo genes in the rat brain. *J. Comp. Neurol.* **442**, 130-155.
- Mizuno, T., Kawasaki, M., Nakahira, M., Kagamiyama, H., Kikuchi, Y., Okamoto, H., Mori, K. and Yoshihara, Y.** (2001). Molecular diversity in zebrafish NCAM family: three members with different VASE usage and distinct localization. *Mol. Cell. Neurosci.* **18**, 119-130.
- Mombaerts, P.** (1999). Molecular biology of odorant receptors in vertebrates. *Annu. Rev. Neurosci.* **22**, 487-509.
- Mombaerts, P., Wang, F., Dulac, C., Chao, S. K., Nemes, A., Mendelsohn, M., Edmondson, J. and Axel, R.** (1996). Visualizing an olfactory sensory map. *Cell* **87**, 675-686.
- Nguyen-Ba-Charvet, K. T., Plump, A. S., Tessier-Lavigne, M. and Chédotal, A.** (2002). Slit1 and Slit2 proteins control the development of the lateral olfactory tract. *J. Neurosci.* **22**, 5473-5480.
- Plump, A. S., Erskine, L., Sabatier, C., Brose, K., Epstein, C. J., Goodman, C. S., Mason, C. A. and Tessier-Lavigne, M.** (2002). Slit1 and Slit2 cooperate to prevent premature midline crossing of retinal axons in the mouse visual system. *Neuron* **33**, 219-232.
- Ressler, K. J., Sullivan, S. L. and Buck, L. B.** (1994). Information coding in the olfactory system: evidence for a stereotyped and highly organized epitope map in the olfactory bulb. *Cell* **79**, 1245-1255.
- Schwartz, G. A., Kostek, C., Ahmad, N., Dibble, C., Pays, L. and Püschel, A. W.** (2000). Semaphorin 3A is required for guidance of olfactory axons in mice. *J. Neurosci.* **20**, 7691-7697.
- Seeger, M., Tear, G., Ferres-Marco, D. and Goodman, C. S.** (1993). Mutations affecting growth cone guidance in *Drosophila*: genes necessary for guidance toward or away from the midline. *Neuron* **10**, 409-426.
- St John, J. A., Clarris, H. J. and Key, B.** (2002). Multiple axon guidance cues establish the olfactory topographic map: how do these cues interact? *Int. J. Dev. Biol.* **46**, 639-647.
- Sundaresan, V., Roberts, I., Bateman, A., Bankier, A., Sheppard, M., Hobbs, C., Xiong, J., Minna, J., Latif, F., Lerman, M. and Rabbitts, P.** (1998). The DUTT1 gene, a novel NCAM family member is expressed in developing murine neural tissues and has an unusually broad pattern of expression. *Mol. Cell. Neurosci.* **11**, 29-35.
- Taniguchi, M., Nagao, H., Takahashi, Y. K., Yamaguchi, M., Mitsui, S., Yagi, T., Mori, K. and Shimizu, T.** (2003). Distorted odor maps in the olfactory bulb of semaphorin 3A-deficient mice. *J. Neurosci.* **23**, 1390-1397.
- Tongiorgi, E., Bernhardt, R. R. and Schachner, M.** (1995). Zebrafish neurons express two L1-related molecules during early axonogenesis. *J. Neurosci. Res.* **42**, 547-561.
- Trevarrow, B., Marks, D. L. and Kimmel, C. B.** (1990). Organization of hindbrain segments in the zebrafish embryo. *Neuron* **4**, 669-679.
- Vassar, R., Chao, S. K., Sitcheran, R., Nunez, J. M., Vossell, L. B. and Axel, R.** (1994). Topographic organization of sensory projections to the olfactory bulb. *Cell* **79**, 981-991.
- Walter, J., Müller, B. and Bonhoeffer, F.** (1990). Axonal guidance by an avoidance mechanism. *J. Physiol.* **84**, 104-110.
- Wang, F., Nemes, A., Mendelsohn, M. and Axel, R.** (1998). Odorant receptors govern the formation of a precise topographic map. *Cell* **93**, 47-60.
- Westerfield, M.** (1995). *The Zebrafish Book*. Eugene, OR: University of Oregon Press.
- Whitesides, J. G., III and LaMantia, A. S.** (1996). Differential adhesion and the initial assembly of the mammalian olfactory nerve. *J. Comp. Neurol.* **373**, 240-254.
- Whitford, K. L., Marillat, V., Stein, E., Goodman, C. S., Tessier-Lavigne, M., Chédotal, A. and Ghosh, A.** (2002). Regulation of cortical dendrite development by Slit-Robo interactions. *Neuron* **33**, 47-61.
- Whitlock, K. E. and Westerfield, M.** (1998). A transient population of neurons pioneers the olfactory pathway in the zebrafish. *J. Neurosci.* **18**, 8919-8927.
- Whitlock, K. E. and Westerfield, M.** (2000). The olfactory placodes of the zebrafish form by convergence of cellular fields at the edge of the neural plate. *Development* **127**, 3645-3653.
- Yeo, S. Y., Little, M. H., Yamada, T., Miyashita, T., Halloran, M. C., Kuwada, J. Y., Huh, T. L. and Okamoto, H.** (2001). Overexpression of a slit homologue impairs convergent extension of the mesoderm and causes cyclopia in embryonic zebrafish. *Dev. Biol.* **230**, 1-17.
- Yeo, S. Y., Miyashita, T., Fricke, C., Little, M. H., Yamada, T., Kuwada, J. Y., Huh, T. L., Chien, C. B. and Okamoto, H.** (2004). Involvement of Islet-2 in the Slit signaling for axonal branching and defasciculation of the sensory neurons in embryonic zebrafish. *Mech. Dev.* **121**, 315-324.
- Yoshida, T., Ito, A., Matsuda, N. and Mishina, M.** (2002). Regulation by protein kinase A switching of axonal pathfinding of zebrafish olfactory sensory neurons through the olfactory placode-olfactory bulb boundary. *J. Neurosci.* **22**, 4964-4972.
- Yuan, W., Zhou, L., Chen, J. H., Wu, J. Y., Rao, Y. and Ornitz, D. M.** (1999). The mouse SLIT family: secreted ligands for ROBO expressed in patterns that suggest a role in morphogenesis and axon guidance. *Dev. Biol.* **212**, 290-306.
- Zallen, J. A., Yi, B. A. and Bargmann, C. I.** (1998). The conserved immunoglobulin superfamily member SAX-3/Robo directs multiple aspects of axon guidance in *C. elegans*. *Cell* **92**, 217-227.